Attitude Estimation Using a Madgwick Filter

Ilya Semenov
University of Maryland
isemenov@umd.edu

Tim Kurtiak
University of Maryland
tkurtiak@terpmail.umd.edu

Nathan Witztum
University of Maryland
nwitztum@terpmail.umd.edu

***Abstract*—The project presents three methods of attitude estimation using a gyroscope estimator, accelerometer estimator, and a Madgwick filter. These attitude estimators are compared to actual orientation as measured by a visual orientation (VICON) system. The results show that the Madgwick filter is the best method of the three considered for estimating attitude.**

I. Problem Statement

This project aims to demonstrate the accuracy of three different attitude estimation methods using a gyroscope algorithm, accelerometer algorithm, and Madgwick filter. Raw sensor data from an ArduIMU+ V2 6DOF IMU is processed and compared to VICON motion capture system data recorded simultaneously. The test data for this project was provided courtesy of the ESE 650: Learning In Robotics course at the University of Pennsylvania

II. Processing Sensor Data

Raw IMU data must be processed in order to gain usable information about the system orientation.

First, gyroscope readings must be scaled to units of radians per second according to equation 1 below [2]. Additionally, gyroscope bias is removed. Gyroscope bias, b_g, is calculated by assuming the IMU is at rest for the first 200 readings after it begins logging data. An average of the gyroscope readings is taken in each axis as the bias for that axis.

$$\underline{w} = \frac{3300}{1023} \cdot \frac{\pi}{180} \cdot 0.3 \cdot (\underline{w}_{raw} - \underline{b}_g) \tag{1}$$

Raw accelerometer data is processed using equation 2 below. This equation differs from the provided accelerometer processing equation as we found that the raw accelerometer reports accelerations in G's and not in m/s^2. As such, an appropriate equation was reverse engineered to process accelerometer data in a realistic magnitude.

$$\underline{a} = (9.81\frac{m}{s^2})(\underline{a}_{raw} \cdot \underline{s}_a + \underline{b}_a) \tag{2}$$

Accelerometer data may further be processed via a low pass filter to remove noise. Additionally, the gyroscope data can be high pass filtered in order to reduce low frequency errors. However, we elected to proceed without filtering to illustrate the pros and cons of each attitude estimation algorithm discussed.

III. Gyroscope Integration Method

Attitude estimation using only a gyroscope can be attained via numerical integration of processed gyroscope data.

The gyroscope reads body rates $\underline{w} = [p, q, r]^T$, which are converted to Euler angle rates for a Z-Y-X transformation with equation 3 [4].

$$\begin{bmatrix} \dot{\phi} \\ \dot{\theta} \\ \dot{\psi} \end{bmatrix} = \begin{bmatrix} 1 & sin\phi tan\theta & cos\phi tan\theta \\ 0 & cos\phi & -sin\phi \\ 1 & sin\phi sec\theta & cos\phi sec\theta \end{bmatrix} \begin{bmatrix} p \\ q \\ r \end{bmatrix} \tag{3}$$

If initial orientation is known, the converted gyroscope readings multiplied by a time increment, Δt, provide an estimate of the change in orientation over that time period. For example, the Euler angle pitch orientation is calculated below.

$$\theta_{t+1} = \theta_t + \dot{\theta}_t \cdot \Delta t \tag{4}$$

Figures 1 through 6 show the gyroscope attitude estimation in orange compared to the VICON actual orientation in blue. The gyroscope attitude tends to capture large changes in orientation very well and accurately tracks rotations in all axes during a short time span. However, over time the gyroscope attitude estimation drifts away from the VICON data due to accruing integration errors and sensor noise. By the end of each dataset, the gyroscope method accrues more than 10 degrees of error compared to the VICON orientation.

IV. Accelerometer Method

In order to estimate attitude using an accelerometer, we must assume that the IMU is only rotating and not linearly accelerating. With this assumption, the gravity vector can be used as a known reference orientation from which to compare the accelerometer data. As such, the calculation of attitude becomes trivial as a set of Euler angle rotations [2] to align the sensor acceleration vector with the known orientation of the gravity vector. Let $\underline{a} = [a_x, a_y, a_z]^T$ for the equations below:

$$\phi = tan^{-1}\left(\frac{a_y}{\sqrt{a_x^2 + a_z^2}}\right) \tag{5}$$

$$\theta = tan^{-1}\left(\frac{-a_x}{\sqrt{a_y^2 + a_z^2}}\right) \tag{6}$$

$$\psi = tan^{-1}\left(\frac{\sqrt{a_x^2 + a_y^2}}{a_z}\right) \tag{7}$$

One issue with this method is the assumption of absence of linear acceleration. In practice, significant linear accelerations may occur when fast movements are executed on a vehicle. In these events, the algorithm will confuse linear acceleration with rotation and calculate an incorrect attitude. Additionally, bias and noise in the accelerometer sensor will add error and uncertainty.

Figures 1 through 6 show the accelerometer attitude estimation in green compared to the VICON actual orientation in blue. The resulting attitude estimation from the accelerometer algorithm above tracked VICON orientation data well in the pitch and roll axis. In the yaw axis, this method did not track orientation well. This is because the observed gravity vector does not perceptibly change when the aircraft is yawed if the vehicle is level. Additionally, the accelerometer attitude estimation shows high frequency jitter caused by sensor noise. The accelerometer sensor would benefit from a low pass filter, but it would also cause the attitude estimation to lag.

V. Madgwick Filter Method

The Madgwick filter combines both accelerometer and gyroscope data to calculate attitude [1]. The algorithm integrates gyroscope rates to capture fast movements as well as the gyroscope method discussed earlier, but also uses the accelerometer to eliminate gyroscopic drift and maintain an accurate and calibrated attitude estimate. The Madgwick filter utilizes quaternions to represent attitude without singularities known as gimbal lock. The filter uses the current state $\underline{q}_t$, where $\underline{q}_t$ represents the quaternion state at time t, along with gyroscope data $\underline{w}_{t+1}$ to find $\dot{\underline{q}}_t$. It is assumed that the initial quaternion attitude state q_0 is known. We first estimate the rate of change based on the gyroscope measurements by equation 8 below:

$$\dot{\underline{q}}_\omega = \frac{1}{2}\underline{q}_t \otimes \begin{bmatrix} 0 \\ \underline{w} \end{bmatrix} \tag{8}$$

Next, the accelerometer data is integrated using a solution to the minimization of the error between the gravity vector and the measured acceleration vector [3]. Let $\underline{q}_t = [p_1, p_2, p_3, p_4]^T$ and $\underline{a}_{t+1} = [a_x, a_y, a_z]^T$ The math has been simplified for implementation below:

$$\nabla f = \begin{bmatrix} -2q_3 & 2q_2 & 0 \\ 2q_4 & 2q_1 & -4q_2 \\ -2q_1 & 2q_4 & -4q_3 \\ 2q_2 & 2q_3 & 0 \end{bmatrix} \begin{bmatrix} 2(q_2q_4 - q_1q_3) - a_x \\ 2(q_1q_2 + q_3q_4) - a_y \\ 2(.5 - q_2^2 - q_3^2) - a_z \end{bmatrix} \tag{9}$$

$$\Delta\underline{q}_a = -\beta\frac{\nabla f}{\|\nabla f\|} \tag{10}$$

β is a tunable parameter which controls the magnitude of accelerometer data to trust in order to counter gyroscope error. For our implementation, a value of $\beta = 0.1$ was used which resulted in a good attitude estimation with minimal overshoot.

Lastly, the accelerometer and the gyroscope rates are combined and integrated over the sampling time Δt to generate an attitude increment which is applied to the previous attitude estimate. The attitude state is thus updated to reflect the gyroscope and accelerometer updates as per equation 11.

$$\underline{q}_{t+1} = \underline{q}_t + (1-\gamma)\cdot\dot{\underline{q}_\omega}\cdot\Delta t + \gamma\cdot\Delta\underline{q}_a \tag{11}$$

where γ is the accelerometer weight factor. In our implementation, a value of $\gamma = 0.1$ is used.

Figures 1 through 6 show the Madgwick filter attitude estimation in red compared to the VICON actual orientation in blue. The Madgwick attitude estimate tracks the VICON data better than all other methods tested.

VI. Results

Figures 1 through 6 below show Z-Y-X Euler angle orientation for each of the 6 test data sets comparing gyroscope, accelerometer, Madgwick, and VICON reported attitudes.

The results of the first 6 datasets were also animated and recorded here:
Dataset 1: https://youtu.be/CguQl12Buag
Dataset 2: https://youtu.be/pbOzvX_zYKg
Dataset 3: https://youtu.be/6zXe_M-81r8
Dataset 4: https://youtu.be/pRfGNeg40PY
Dataset 5: https://youtu.be/GPoBwnvKR-E
Dataset 6: https://youtu.be/ns9sPc0w3yI

Additionally, test data sets 7 through 10 are shown in Figures 7 through 10. These data sets do not have VICON data as comparison.

VII. Lessons Learned

The Madgwick filter does not accrue error over time like the gyroscope method, but still tracks fast changes in orientation well. In certain data sets, such as the one shown in Figure 6, the Madgwick filter is affected by high frequency noise. Additionally, it was susceptible to small amounts of yaw axis drift over time due to the low ability of the accelerometer to correct yaw axis errors.

It should be noted that there exists a constant phase shift between the VICON attitudes (in blue) and all IMU derived attitudes. The soft-synchronization appears to present a constant lag between the VICON and IMU data timestamps. While this problem was ignored during our analysis, an automatic syncing of the timestamps may be completed for better plots and data presentation.

Throughout this project the limitations of Euler angles in describing attitude orientation have repeatedly presented themselves. The VICON data was given in $3x3$ rotation matrix format, allowing two possible sets of Euler angles, and assumption had to be made to pick one set. Converting body rates and quaternions to Euler angles is cumbersome and error prone. Our group spent a significant amount of time debugging such issues. Additionally, gimbal lock is possible with Euler angles, observed as large jumps in orientation angles when that angle nears 90°, as seen in Figure 1. Overall it is much simpler

to work with quaternions to avoid problems with representing Euler angles.

Lastly, this project was conducted to illustrate the effects of different attitude algorithms on raw sensor data. For future implementations it is recommended to utilize a high pass filter for the gyroscope and a low pass filter for the accelerometer. These filters may help reduce noise in the signals and allow the gyroscope and accelerometer to work better in each one's area of strength.

VIII. Conclusion

Overall, the Madgwick filter outperformed the gyroscope and accelerometer methods of attitude estimation. The Madgwick filter does not experience drift like the gyroscope and responds to fast changes in attitude better than the accelerometer. In this way, the Madgwick filter combines the best features of the accelerometer and gyroscope to estimate attitude with less error than each alone. However, the Madgwick filter does still experience some error and does not perfectly track attitude, particularly due to drift in the yaw axis.

References

[1] Sebastian OH Madgwick, Andrew JL Harrison, and Ravi Vaidyanathan. "Estimation of IMU and MARG orientation using a gradient descent algorithm." 2011 IEEE international conference on rehabilitation robotics. IEEE, 2011.

[2] https://prgaero.github.io/2019/proj/p1a/report

[3] *https://www.x-io.co.uk/res/doc/madgwick_internal_report.pdf*

[4] *http://www.stengel.mycpanel.princeton.edu/Quaternions.pdf*

IX. Figures

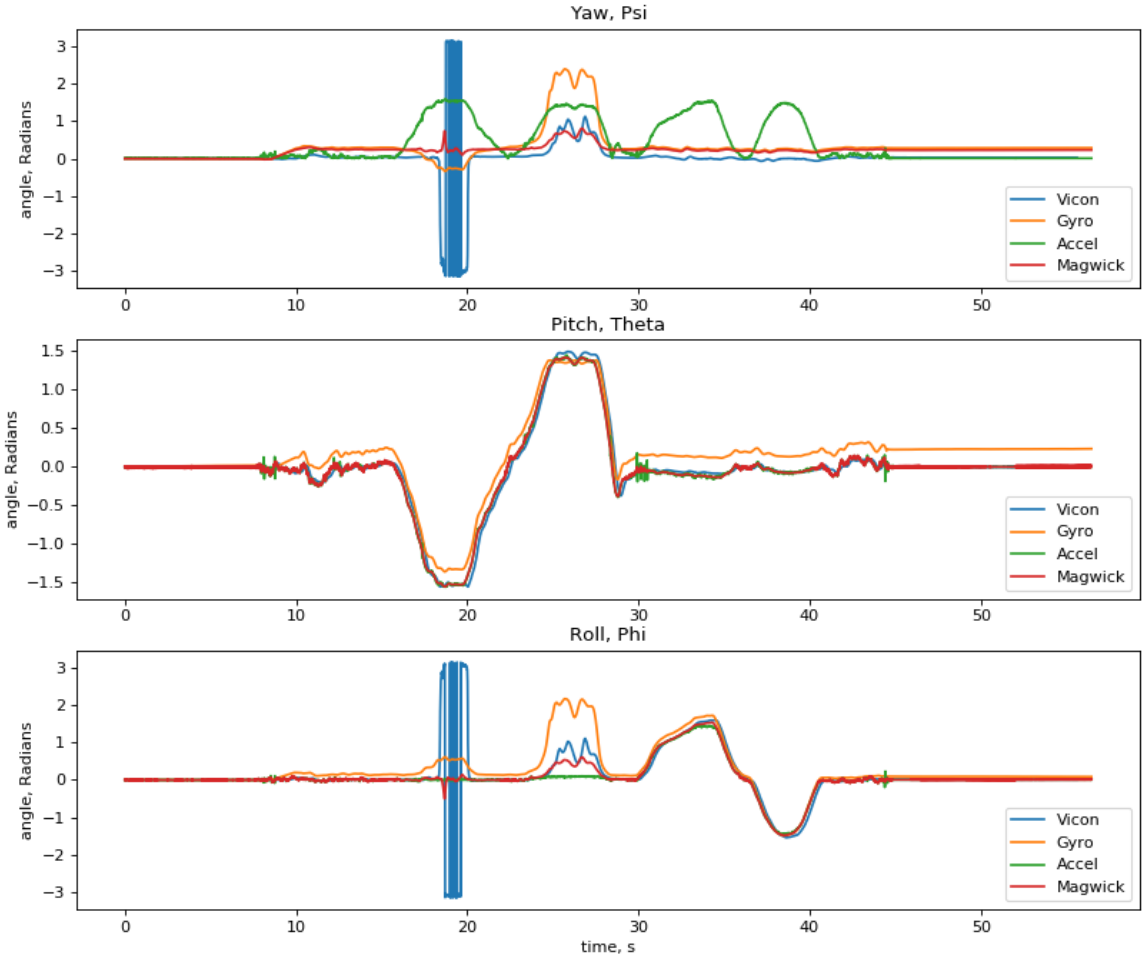

Figure 1. Euler Angle Plots for Test Data Set 1

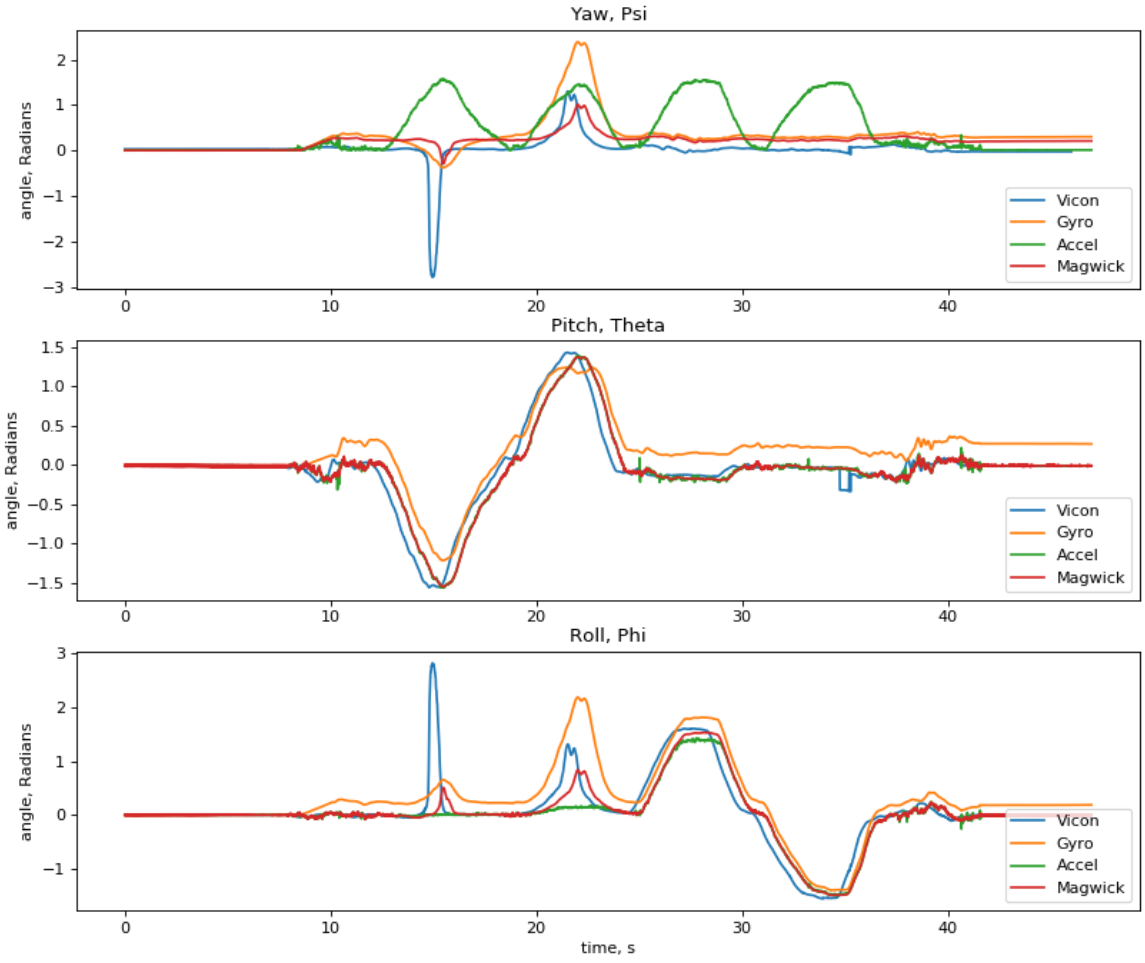

Figure 2. Euler Angle Plots for Test Data Set 2

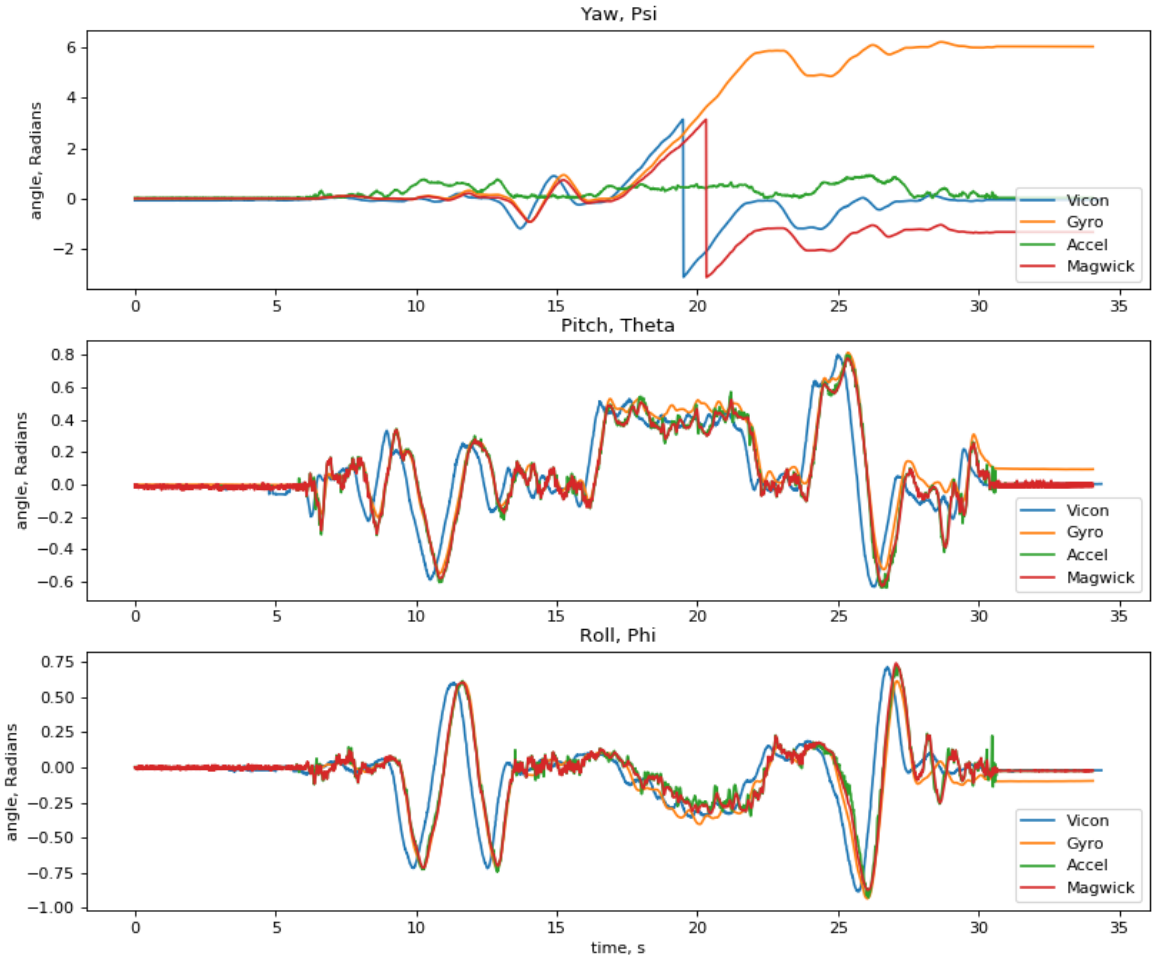

Figure 3. Euler Angle Plots for Test Data Set 3

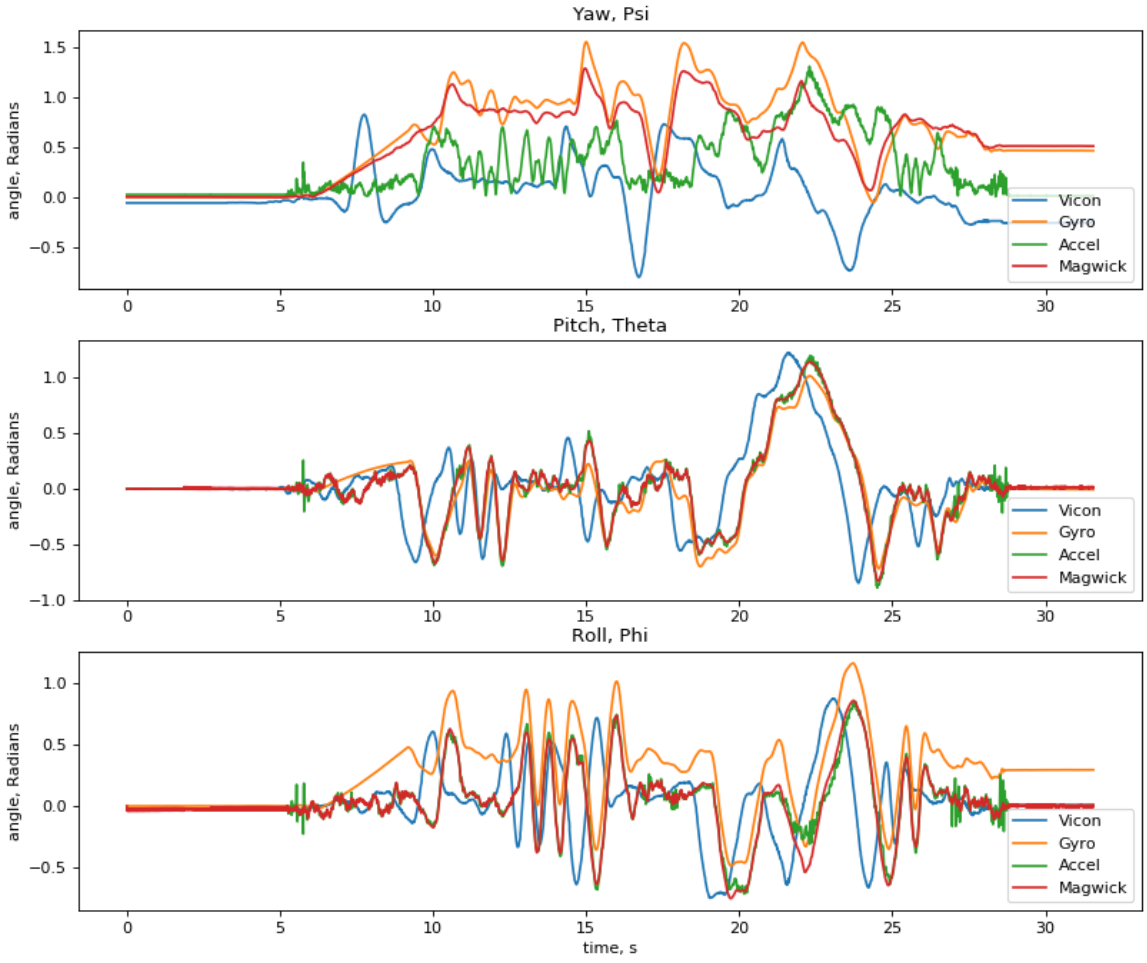

Figure 4. Euler Angle Plots for Test Data Set 4

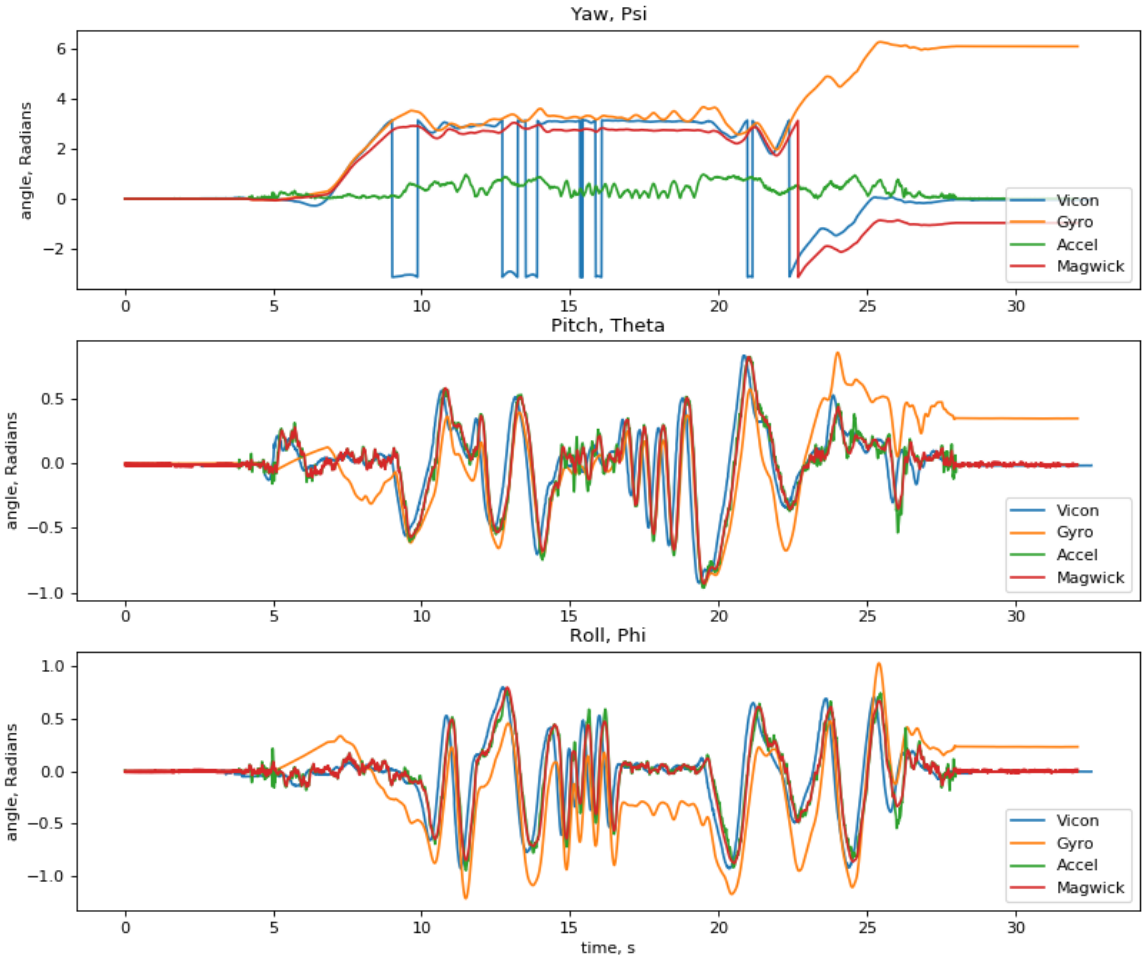

Figure 5. Euler Angle Plots for Test Data Set 5

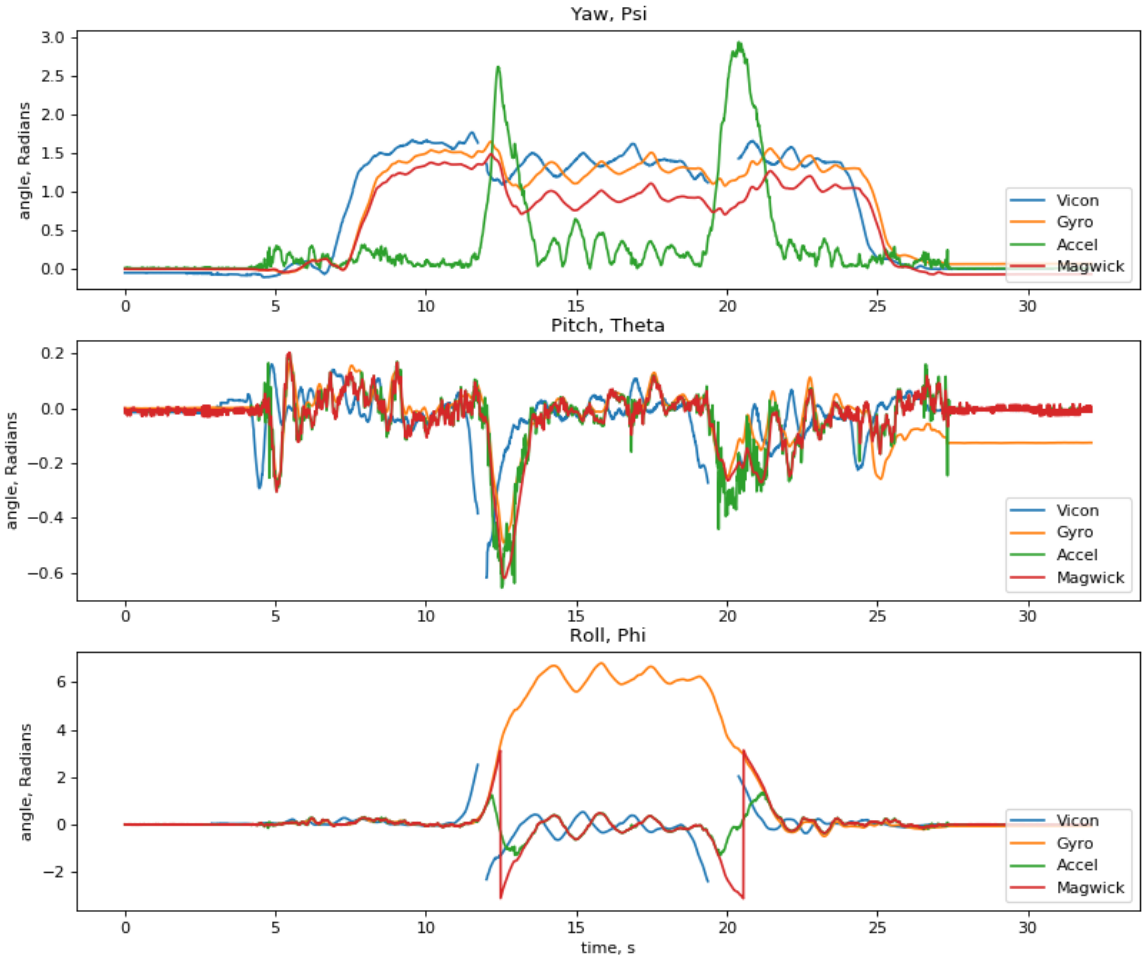

Figure 6. Euler Angle Plots for Test Data Set 6

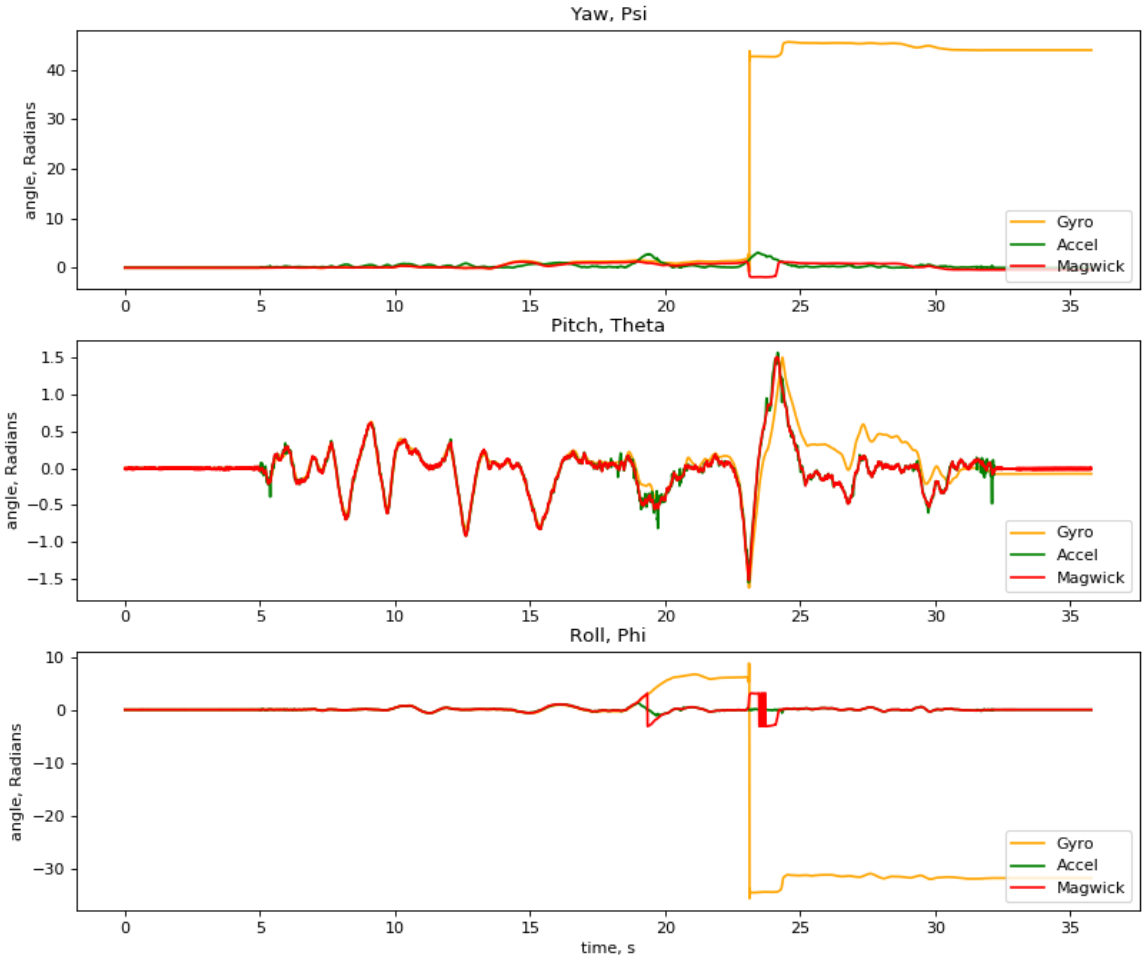

Figure 7. Euler Angle Plots for Data Set 7 - No VICON data included

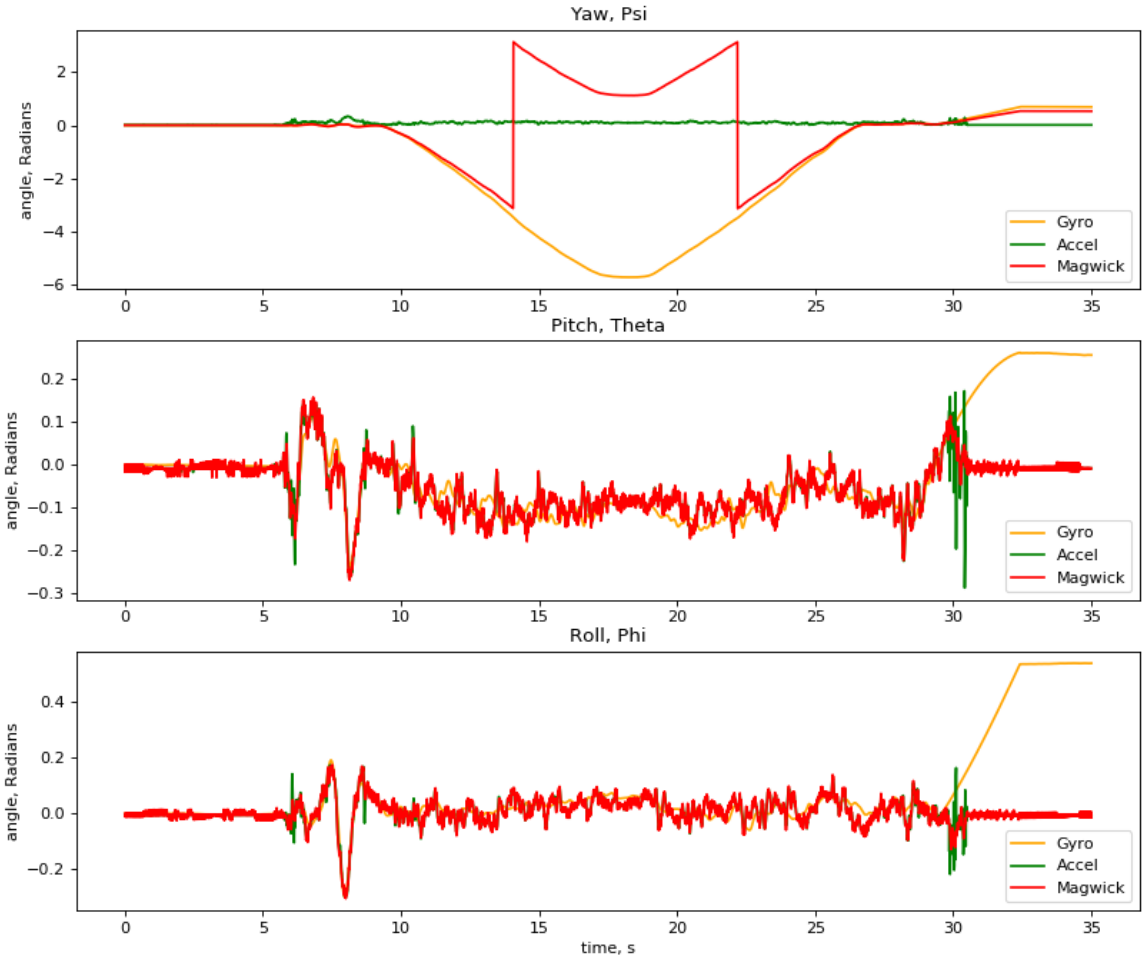

Figure 8. Euler Angle Plots for Data Set 8 - No VICON data included

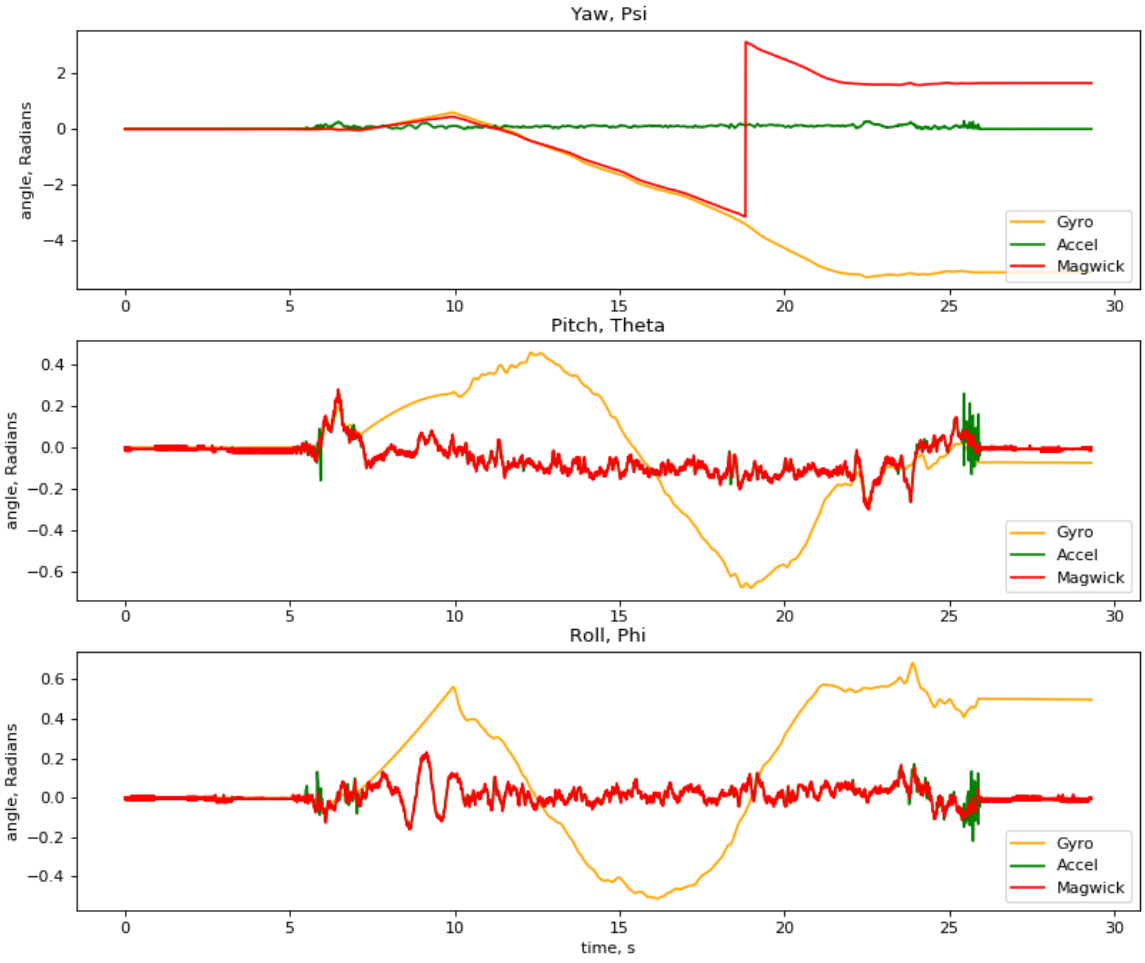

Figure 9. Euler Angle Plots for Data Set 9 - No VICON data included

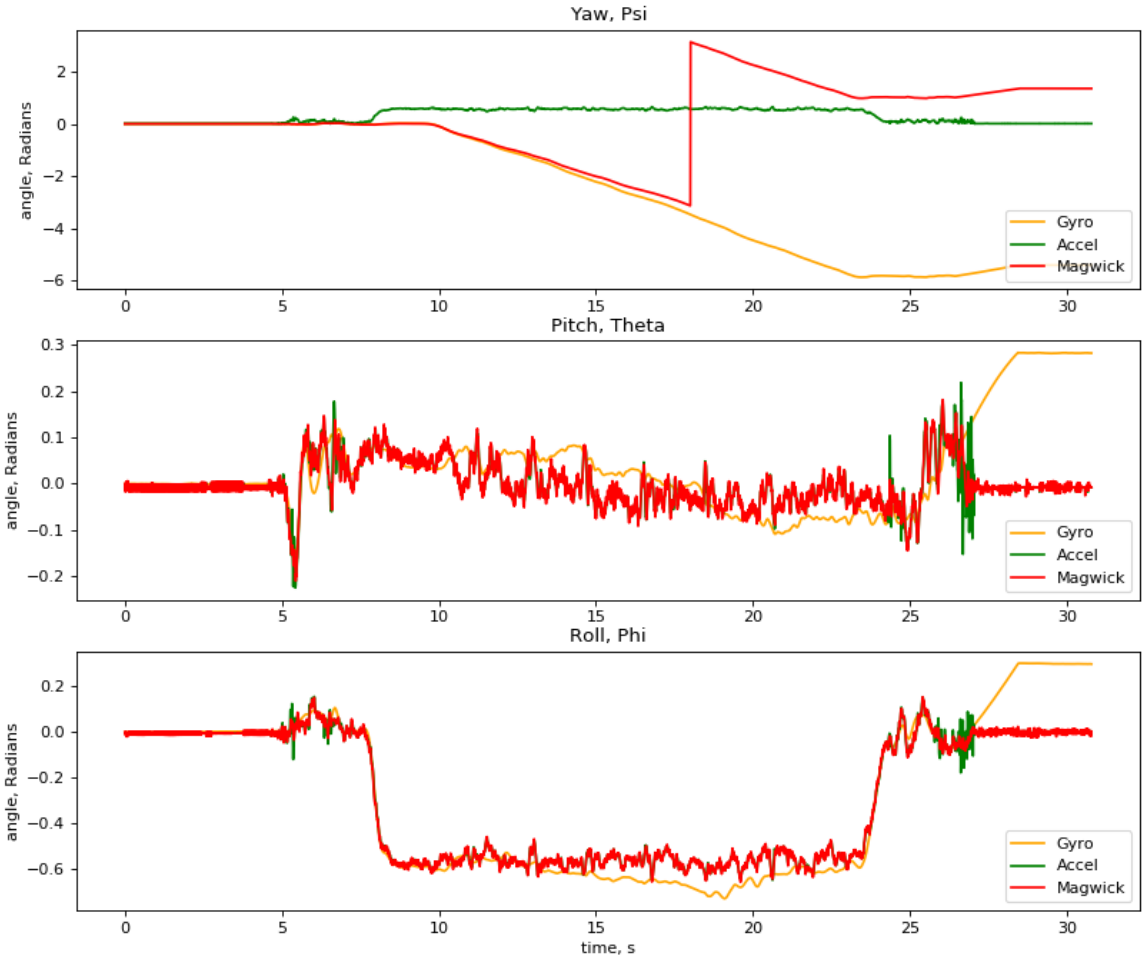

Figure 10. Euler Angle Plots for Data Set 10 - No VICON data included